

# Magazine of Civil Engineering

ISSN 2712-8172

journal homepage: http://engstroy.spbstu.ru/

Research article UDC 69.04

DOI: 10.34910/MCE.132.2



# Bearing capacity of lightweight steel concrete enclosure wall panels

V.A. Rybakov<sup>1</sup> , K. Usanova<sup>1</sup> , A.V. Seliverstov<sup>2</sup>, A.A. Kislitcyna<sup>1</sup>, A.A. Tsvetkova<sup>1</sup>, S.V. Akimov<sup>1</sup>

☑ fishermanoff@mail.ru

**Keywords:** lightweight steel concrete enclosure wall panels, fastenings, bearing capacity, self-tapping screw

Abstract. The object of this study is lightweight steel concrete enclosure wall panels consisting of light gauge steal profiles and foam lightweight cellular concrete filling in general and, in particular, their fastenings. The purpose of this study is to develop a methodology for calculating enclosure wall LSCS panels with partial resting on floor slabs fastened with self-tapping screws of the Harpoon type. Methods. The experimental study of behaviour of the sample of the LSCS panel fastened via galvanized plate with self-tapping screws to a metal tube, the rigidity of which is many times higher than the rigidity of the LSCS panel, from the action of a distributed load simulating wind pressure, is carried out. The density of foam concrete of the panel was measured during experiment and amounted to 370 kg/m3. Results. The methodology of calculating the bearing capacity of LSCS panel-to-slab fastenings is proposed and substantiated. The analytically calculated destructive load 28.25 kN is 9.3 % less than experimentally obtained destructive load 30.9 kN. It is shown that the loss of load-bearing capacity of the panel happens due to bearing of the steel sheet of the web of the light gauge steel profile of the panel. It is shown that the rigidity of the LSCS panel fastenings varies from the one corresponding to the fixed-support calculation scheme to the one corresponding to the hinged-support calculation scheme. The behaviour of the panel corresponds to the fixed-support calculation scheme before the load is 30 % of the value that gives the maximum allowable deflection, then the fasteners work as a finite stiffness support and turn into a plastic hinge when the load reaches 90 % of the abovementioned load. It is proposed to use the hinged-support calculation scheme in design practice.

**Funding:** The research was carried out with the support of the Russian Science Foundation grant, https://rscf.ru/project/23-29-00564/

**Citation:** Rybakov, V.A., Usanova, K., Seliverstov, A.V., Kislitcyna, A.A., Tsvetkova, A.A., Akimov, S.V. Bearing capacity of lightweight steel concrete enclosure wall panels. Magazine of Civil Engineering. 2024. 17(8). Article no. 13202. DOI: 10.34910/MCE.132.2

#### 1. Introduction

Energy efficiency concerns are critical in modern construction, and therefore, the choice of an optimal wall structure plays an important role.

The most common technologies for producing enclosing structures can be divided into prefabricated structures and those constructed on site. The main disadvantage of structures built directly on site is the low speed of erection. Prefabricated structures are free from this disadvantage: prefabricated reinforced concrete panels, sheathed cold-formed steel (CFS) panels, and lightweight steel-concrete structural panels

© Rybakov, V.A., Usanova, K., Seliverstov, A.V., Kislitcyna, A. A., Tsvetkova, A.A., Akimov, S.V., 2024. Published by Peter the Great St. Petersburg Polytechnic University.

<sup>&</sup>lt;sup>1</sup> Peter the Great St. Petersburg Polytechnic University, St. Petersburg, Russian Federation

<sup>&</sup>lt;sup>2</sup> LLC "Sovbi", St. Petersburg, Russian Federation

(LSCS panels), consisting of LSCS (lightweight steel concrete structures). Thanks to factory assembly of panels, the labour intensity of their installation is reduced by 60% compared to the labour intensity of installing, for example, ventilated facades [1]. Moreover, prefabricated structures help reduce heating and cooling costs of the building [2].

External reinforced concrete wall panels typically consist of three layers: a load-bearing reinforced concrete layer, a middle thermal insulation layer, and an external protective reinforced concrete layer. The panels are connected to each other through embedded parts by welding or using key joints on reinforcement bar protrusions. High speed and low cost of construction as well as low cost of interior decoration due to smooth-faced walls make this technology attractive [3]. However, the low thermal insulation capacity of reinforced concrete, its high specific weight requiring the use of a crane, are obstacles to the use of this type of enclosing structures in low-rise construction.

Another type of enclosing structure is sheathed CFS panels – a multilayer structure consisting of a frame filled with insulation and clad with facing sheets [4]. One of the significant disadvantages of frame-sheathed walls is the flammability of mineral wool insulation, which reduces the fire resistance of the wall panel and limits the scope of application for this type of enclosing structure.

The third type of prefabricated structures is LSCS panels, consisting of light gauge steel profiles (LGSPs) and foam lightweight cellular concrete (LCC). The Fig. 1 shows a drawing of one type of this panel. These structures can serve both load-bearing and enveloping functions in buildings and are free from the aforementioned disadvantages. Construction of a two-story house from LSCS panels takes only 15 days. Photo on Fig. 2 shows a detached residential house made from LSCS panels on the 5<sup>th</sup> and 15<sup>th</sup> day of construction.

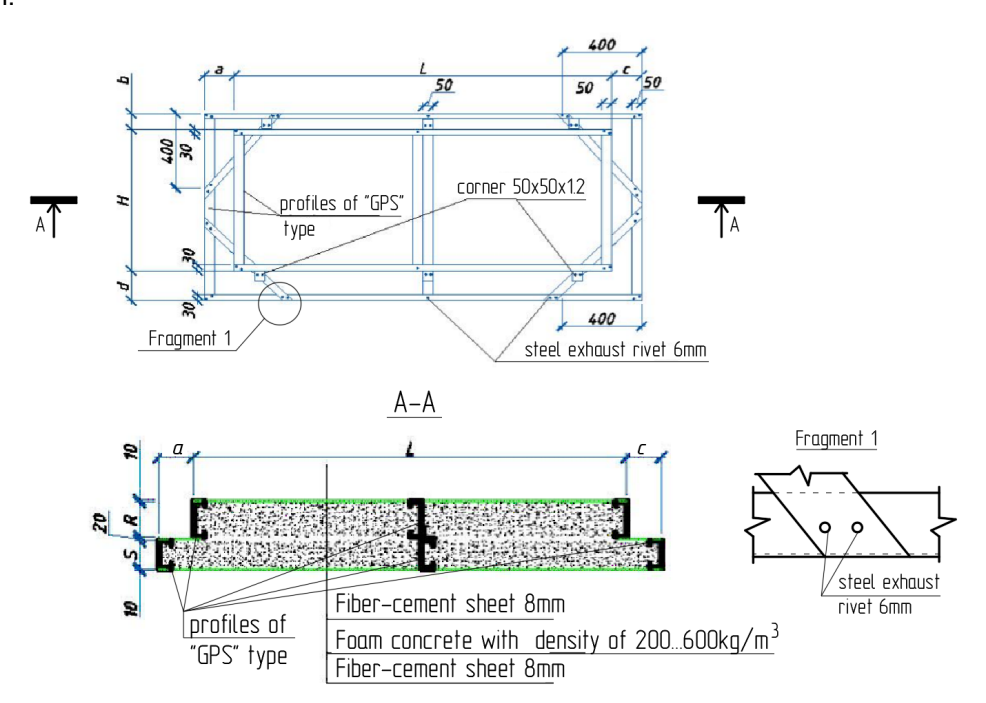


Figure 1. Composition of the wall panel and the general view.



Figure 2. a) Mounted panels of a LSCS house on the 5<sup>th</sup> day of construction; b) Finished house on the 15th day of construction.

The LSCS were described for the first time in [5]. It is based on constructing a structure from lightweight thin-walled steel profiles and filling the space between them with foam LCC .Prefabricated LSCS panels are a specific case of a structure built using LSCS technology.

When concrete and steel structures work together, the combined properties of the system exceed the sum of the individual properties of concrete and steel considered separately. This phenomenon is observed under various types of stress-strain conditions, such as deformations caused by temperature changes [6], cyclic loading [7], concentric [8, 9] and eccentric [10] compression, and bending [11].

Concrete, when working in combination with the steel structure, significantly increases both its local and overall stability [12, 13]. The fact of increased stability in composite LGS structures is also substantiated in the experimental study in [14], where the compressed chord of LGS truss was filled with concrete. Similarly, Jiqin Wang and his research team [15] conducted experimental studies on LGS and foam concrete panels under cyclic loading.

It has been experimentally proven that foam concrete, despite its extremely low strength class, actually contributes to structural performance, preventing effects, such as local buckling, failure, and warping of the steel profile elements [16]. Additionally, it increases the overall load-bearing capacity of the flooring by 20–25 % [5]. Study [17] established that the shear strength of a lightweight concrete sample is approximately the same as that of a sample made from regular concrete.

Foam concrete in the structure serves as a thermal and sound insulation material [18], and due to its adhesion to steel, it increases the load-bearing capacity of LGS profiles, preventing profile distortion and ensuring that there is no cross-sectional warping or bimoment, which are integral factors to the mechanics of thin-walled members and often lead to a twofold increase in stresses in the structure. In previous studies, the authors confirmed that the use of foam concrete allows for an increase in the structural performance factor [19]. Similar results were obtained for LGS profiles sheathed with oriented strand boards (OSBs) in [20].

The advantages of composite steel and concrete structures include improved fire resistance compared to steel structures [21–23], reduced steel intensity [24], and increased corrosion resistance [25].

However, in the regulatory documentation governing the use of LGS profile fasteners, there are no recommendations for calculating the fastening of LSCS panels to the load-bearing frame of the building, despite the practicality of using this type of structure, which complicates their design. Some studies, for example [26], reveal that failure of self-tapping screws is the most probable cause of LSCS structural failure. However, there are very few publications in the scientific literature specifically dedicated to the bearing capacity of self-tapping screws in LSCS [27, 28]. The few existing studies [29, 30], and [31] focus on the use of self-tapping screws for fastening LGS profiles to each other.

In light of the above, the aim of this study was formulated: to develop a method for calculating enclosure wall LSCS panels with partial resting on floor slabs fastened with self-tapping screws. To achieve this aim, the following tasks were set:

- 1. Experimental determination of behavior, load-bearing capacity and deflections of a sample of LSCS panel with density of foam concrete 370 kg/m<sup>3</sup>.
- 2. Analytical calculation of the load-bearing capacity of self-tapping screws fastening LSCS panels.
- 3. Calculation of the deflections of LSCS panels for both hinged and rigidly fixed panel supports.
- 4. Assessment of the impact of the fasteners on the calculation scheme.

### 2. Materials and Methods

Fig. 3 shows a constructive solution of supporting the enclosing wall panels on the building's load-bearing structures.

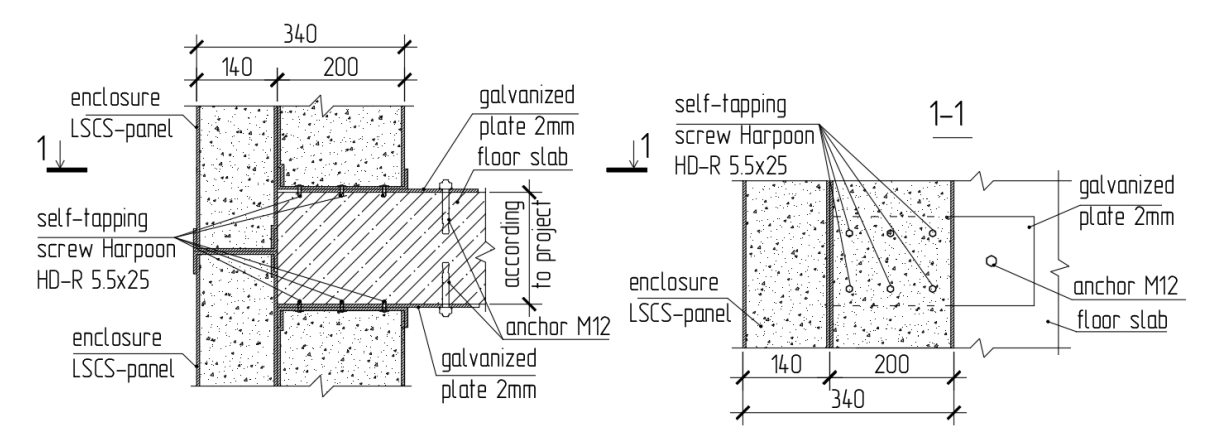


Figure 3. Fastening of the LSCS panel to a floor slab.

Let us model this type of panel support in an experimental study with the following assumption:

- the actual structure is analogous to the tested sample, preserving a 1:10 thickness-to-length ratio;
- the stiffness of the floor slab significantly exceeds that of the LSCS panel. Therefore, for the purposes of testing, the complex-to-manufacture floor slab will be replaced with a 150×150×8 mm profile steel tube;
- due to the constraints of the experimental setup, the test will be performed on a sample measuring 1500×360×170 mm, rather than a full-size panel.

Here is the description of the most important parts of the tested sample:

- self-tapping screws Harpoon HD-R 5.5x25 produced according to Organization Standard STO 0065-83135335-2014 Self-Tapping and Self-Drilling Screws for Wall and Roof Mounting Structures Made of Light Gauge Steel (https://www.snabmetiz.ru/UserFiles/Image/\_Docs/STO\_0065-2014\_Harpoon.pdf) to fix the panel to the 150×150×8 profile steel tube;
- 2 pieces of galvanized mounting plates 120×290×2 mm made of steel with yield stress 275 MPa to fix the panel to the 150×150×8 mm profile steel tube;
- fiber-cement sheets 1500×360×8 mm at both sides of the panel;
- the LSCS frame of the panel made of "GPS-type" profiles 150×50×1.5 mm and filled with foam concrete with the density of 370 kg/m³;
- steel exhaust rivets to fix the elements of the LSCS frame to each other.

The sample was suspended from mounting plates attached to the load-bearing components of the setup and subjected to 4 forces spaced 300 mm apart, which can be considered as an approximation of a distributed load simulating wind pressure.

Here is the description of the most important parts of the experimental setup:

- channel bar 120 mm high, 650 mm long;
- channel bar 120 mm high, 400 mm long, 2 pieces;
- concrete prisms 360×100×100 mm with the density of 2500 kg/m³, 4 pieces;
- wood block filler 360×100×25 mm placed under concrete prisms to prevent local deformation of the steel profile under compression, 4 pieces;
- flexometers, 4 pieces, were placed in the middle of the panel and near the supports;
- hydraulic jack;
- hand-force hydraulic pump;
- dynamometer.

Table 1 shows the characteristics of the equipment.

Table 1. Equipment used for LSCS panel testing.

No	Designation of equipment	Brand	Vendor
1	Hydraulic equipment loading		
	Universal single-sided jack 50 tnf-150 mm	Enerpred	JSC Industrial group Hydromechanics
	Hand-force hydraulic pump 2 l	Enerpred	JSC Industrial group Hydromechanics
2	Compression dynamometer	Stroypribor	LLC Stroypribor
3	Flexometer	Stroypribor	JSC Industrial group Hydromechanics

Fig. 4 shows the configuration of the sample and the experimental setup. The total weight of the distribution system was 1.02 kN.

The tests were conducted on five panel samples.

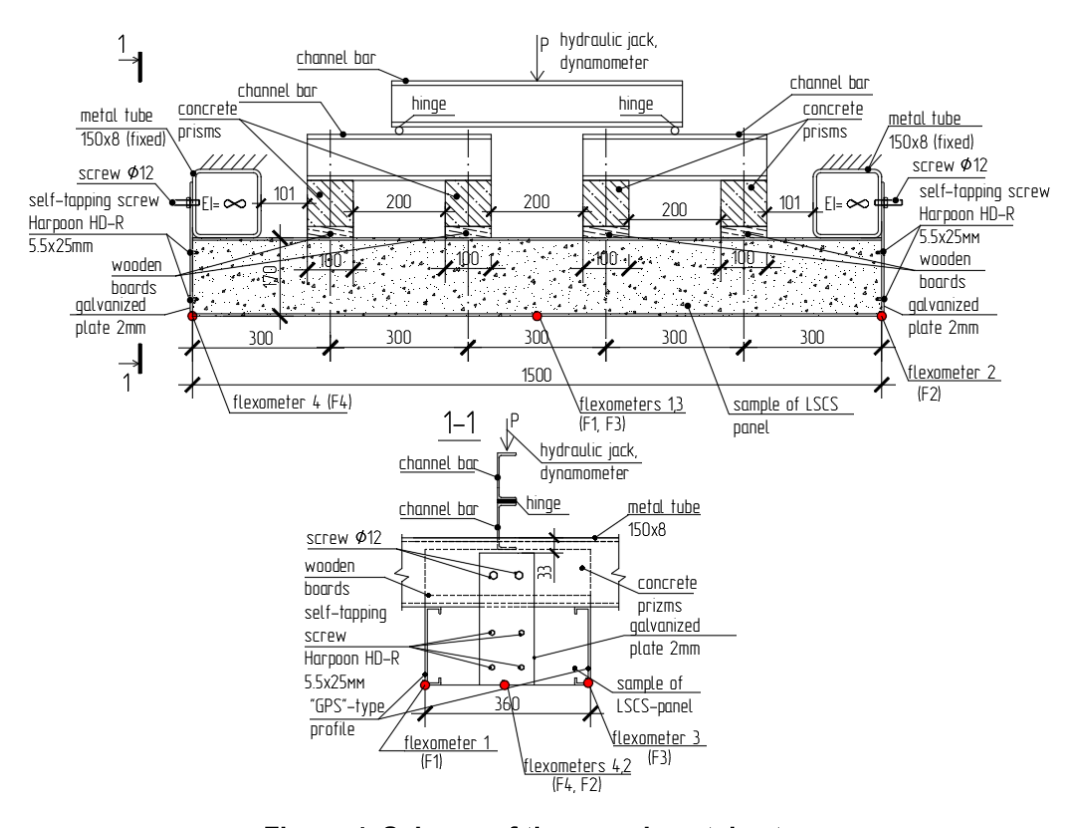


Figure 4. Scheme of the experimental setup.

The loading scheme adopted in the experimental study of the LSCS panel is shown in Fig. 5.

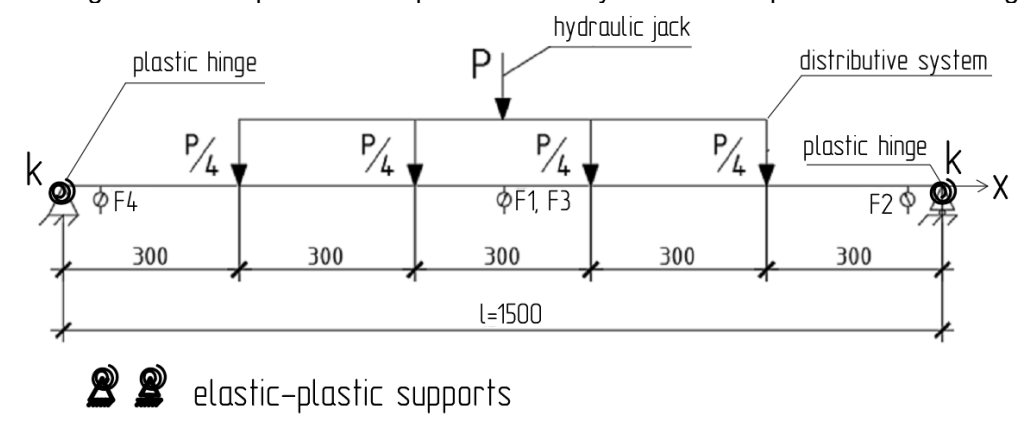


Figure 5. Loading scheme.

Photographs of the experiment and the fastening node before load application are presented in Figs. 6 and 7.

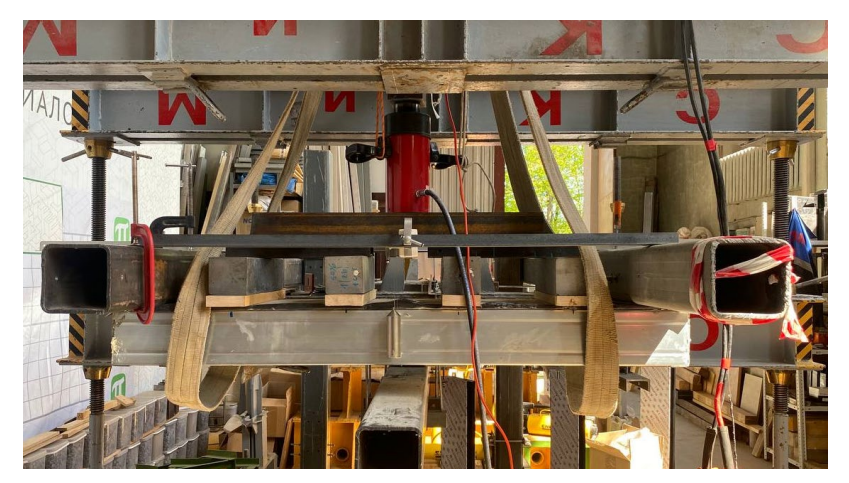


Figure 6. Experimental setup before the start of the test.

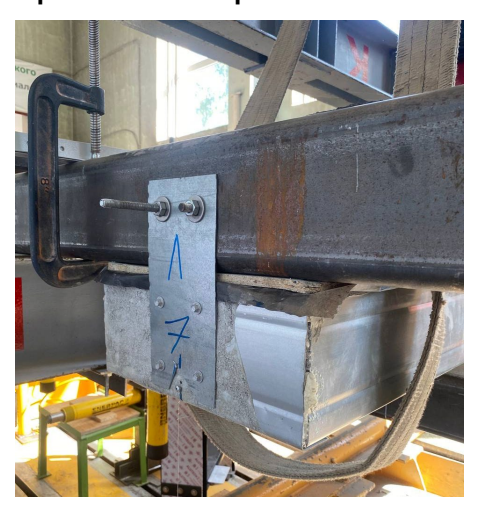


Figure 7. Fastening of the panel before the start of the test.

## 3. Results and Discussion

Figs. 8 and 9 show the nature of the sample failure.

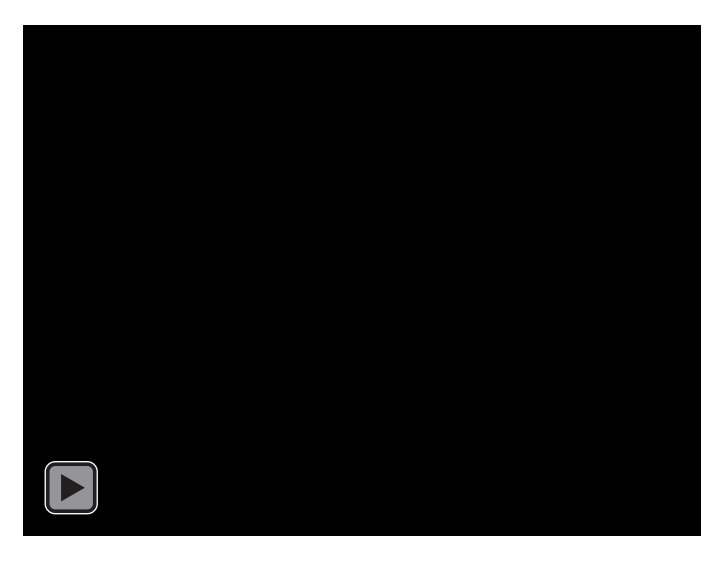


Figure 8. The process of the fastening of the panel failure. Side view. (For watching the video open the PDF in Adobe Acrobat and allow multimedia and 3D content.

DOI: https://doi.org/10.18720/SPBPU/2/VIDEO/z24-21).

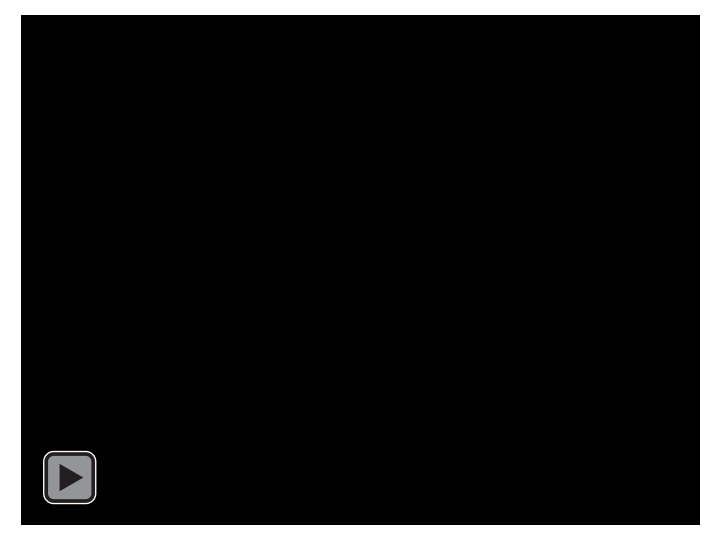


Figure 9. The process of the fastening of the panel failure. Front view. (For watching the video open the PDF in Adobe Acrobat and allow multimedia and 3D content.

DOI: https://doi.org/10.18720/SPBPU/2/VIDEO/z24-20).

Table 2 shows values of the destructive loads for each sample.

Table 2. Destructive load values.

Sample designation	Destructive loads, kN
Panel No 1	31.39
Panel No 2	31.39
Panel No 3	31.39
Panel No 4	33.35
Panel No 5	27.47
Panel No 6	30.41
Average destructive load	30.9

Let us compare the value of the destructive load for the fasteners obtained in the experiment with the values of the destructive load calculated according to STO 0065-2014.

There are three types of connection failures for self-tapping screws subjected to shear:

- sheet bearing;
- sheet tearing along the net section;
- screw shear.

Let us determine the connection strength for each of the three types of connection failures.

The bearing strength of the base material by the screw is calculated by using formula (1):

$$F_b = \frac{\gamma_c \cdot \alpha \cdot R_{un}}{\gamma_m \cdot d \cdot t},\tag{1}$$

where  $F_b$  is design bearing strength of the base material;  $R_{un}$  is ultimate tensile strength of the base material in which the screw is installed;  $\gamma_m$  is safety factor for material strength equal to 1.25;  $\gamma_c$  is condition load effect factor equal to 0.8; t is thickness of the thinner of the connected sheets; d is nominal diameter of the screw,  $\alpha$  is coefficient depending on the thickness ratio of the connected sheets and equal to 1.76.

Shear strength of the screw is calculated using formula (2):

$$F_{v} = \gamma_{c} \cdot \frac{F_{vn}}{\gamma_{m}},\tag{2}$$

where  $F_{v}$  is design shear strength of the screw;  $F_{vn}$  is screw strength according to the manufacturer's standard;  $\gamma_{m}$  is safety factor for material strength equal to 1.3;  $\gamma_{c}$  is condition load effect factor equal to 0.8.

Tensile strength of the sheet along the net section is determined using formula (3):

$$F_t = \gamma_c \cdot \frac{R_{yn}}{\gamma_m} A_{netto}, \tag{3}$$

where  $F_t$  is design tensile strength of the sheet along the net section;  $R_{yn}$  is yield strength of the material in which the self-tapping screw is installed;  $\gamma_m$  is safety factor for material strength equal to 1.25;  $\gamma_c$  is condition load effect factor equal to 0.9;  $A_{netto}$  is net section area of the connected elements.

Table 3 shows the results of the calculation.

Table 3. Destructive load for one self-drilling screw.

Type of connection failure	Destructive load per screw, kN
Sheet bearing	28.25
Sheet tearing along the net section	151.08
Screw shear	40.63

As we can see, the minimum destructive load for this fastener is the load that leads to the bearing failure of the sheet material. It amounts to 28.25 kN, which is 9.3 % less than 30.9 kN, the average destructive load according to the experimental results. The difference in the results is explained by the safety factors in the calculation formula. Thus, this method for determining the strength of the LSCS panel fastening to the floor slab can be considered reliable.

# 3.1. Displacements in the span

Deflections of the panel are determined as the difference between the average readings of deflectometers T1, T3, installed in the middle of the span, and deflectometers T2, T4, installed near the supports.

Let us analytically determine displacements for the hinged (Figs. 10, 11) and fixed on both ends (Fig. 12) calculation models.

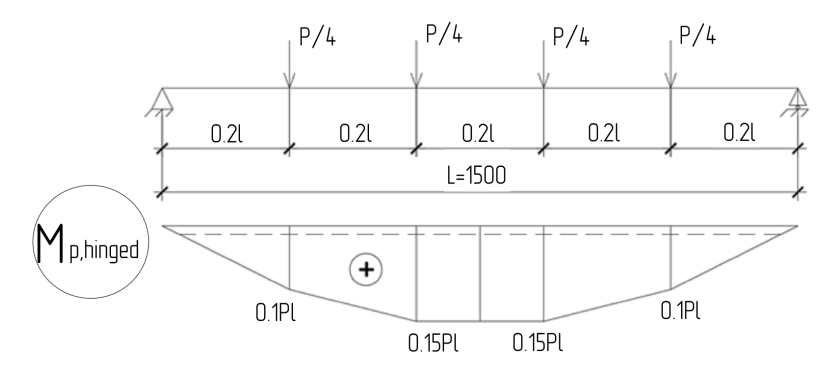


Figure 10. Bending moments in the hinged calculating model.

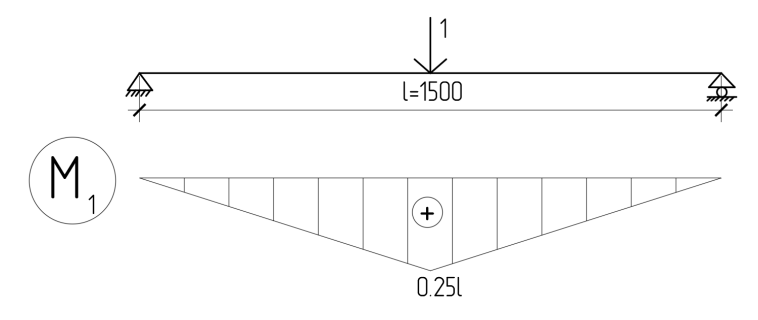


Figure 11. Auxiliary loading.

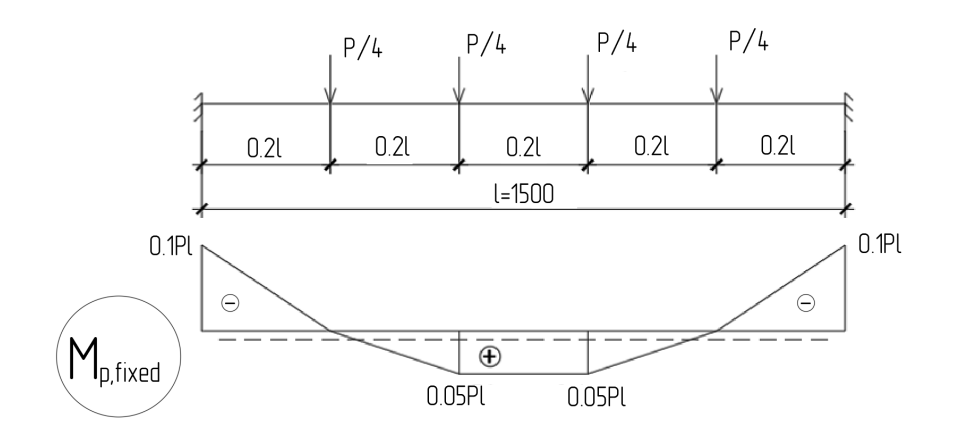


Figure 12. Bending moments in the rigidly fixed calculation model.

Displacements in the hinged model are determined by integration (4):

$$d_{hinged} = \int_{0}^{l} \frac{M_{p,hinged} M_1}{EI} dx = 0.01575 \frac{Pl^3}{EI},$$
 (4)

where  $M_{p, hinged}$  is shown on Fig. 9,  $M_1$  is shown on Fig. 10.

The Maxwell–Mohr integral (4) is obtained by multiplying the  $M_{p,hinged}$  epure (Fig. 10) and  $M_1$  (Fig. 11) using the Simpson formula (formula of parabolic trapezoids).

The bending stiffness of the beam is determined as the sum of the bending stiffnesses of the thin-walled profile and the foam concrete is determined by the formula (5):

$$EI = E_b I_b + E_s I_s = 691 \cdot \text{kN} \cdot \text{m}^2, \tag{5}$$

where  $E_b$  = 843 MPa – modulus of elasticity of the panel is taken according to Organization Standard (LLC Sovbi, Russian Federation) STO 06041112.002-2018 "Steel-Concrete structures made of thermal insulation non-autoclave foam concrete profile steel cladded with fiber cement sheets" (STO 06041112.002-2018), a density of 370 kg/m³, determined by weighing the panels after the experiment;  $I_b$  = 1.47·10<sup>4</sup>cm<sup>4</sup> – moment of inertia of the panel;  $E_s$  = 2.1·10<sup>5</sup> MPa – modulus of elasticity of steel;  $I_s$  = 282 cm<sup>4</sup> – moment of inertia of two GPS-type profiles fabricated according to STO 06041112.002-2018. This document was developed on the basis of the research, conducted by us in 2018-2023 years [5, 21, 25].

Similarly, we obtain the formula for determining the displacements in the middle of the span in the fixed-supports model through integration (6):

$$d_{fixed} = \int_{0}^{l} \frac{M_{p,fixed} M_1}{EI} dx = 0.00325 \frac{Pl^3}{EI},$$
 (6)

where  $\boldsymbol{M}_{p, hinged}$  is shown on Fig. 12,  $\boldsymbol{M}_1$  is shown on Fig. 11.

The Maxwell–Mohr integral (6) is obtained by multiplying the  $M_{p,hinged}$  epure(Fig. 12) and  $M_1$  (Fig. 11) using the Simpson formula (formula of parabolic trapezoids).

For the nonrigid fastening of the walls of a multi-storey building within one floor, the maximum horizontal deflection of the concerned panel as of a separate structural element is calculated by formula (7):

$$f_u = \frac{h_s}{300} = \frac{1500}{300} = 5 \text{ mm},$$
 (7)

where  $h_{\rm s}$  – the hight of the storey (in our research it is the length of the panel l=1500 mm).

The stresses in the tested sample were found to be 200 MPa for the hinged system and 65 MPa for rigidly fixed system, and they do not reach the yield strength of the steel which equals 220 MPa. The limitation of the profile operation happens due to exceeding the maximum deflection.

To conclude the study, let us examine the experimental deflection values and compare them with the calculated values. The results are presented in Fig. 13.

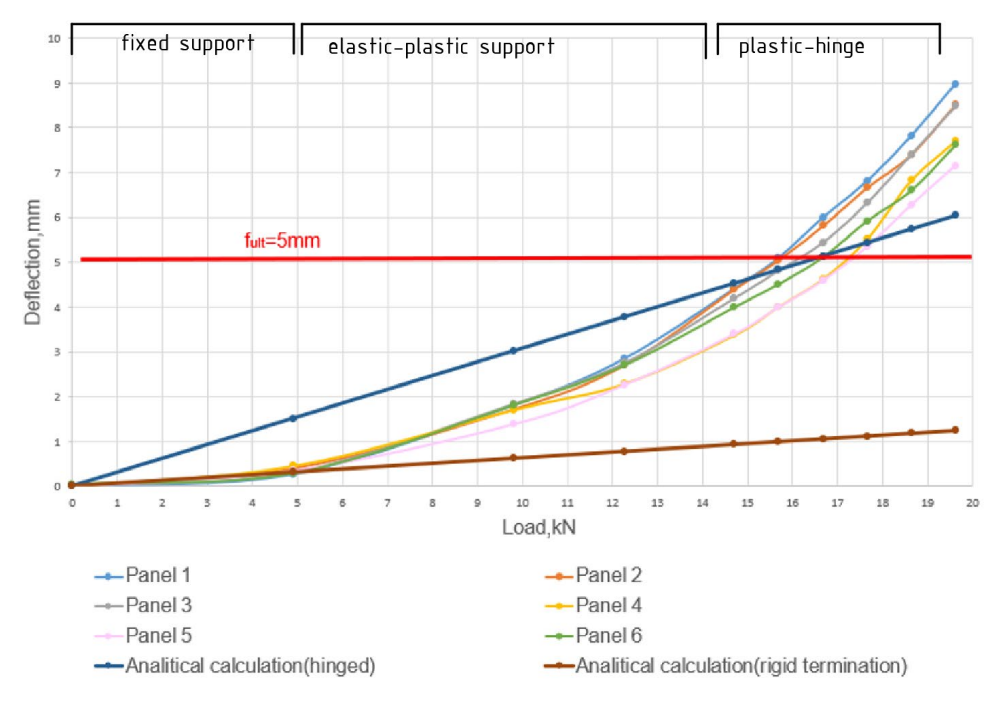


Figure 13. Deflection-load diagram.

We can observe a change in the behaviour of the panel. Initially, when the load is between 0 and 4.9 kN, the behaviour of the panel corresponds to that of a beam rigidly fixed on both ends. As the load increases, plastic hinges begin to form at the supports, and the behaviour of the specimen shifts toward that of a beam with hinged supports. Since the plastic hinges do not form instantaneously but over time, the behaviour of the structure changes gradually and is nonlinear. For the same reason, the deflection values of the panel from the applied load, as determined experimentally, are lower than those determined analytically for the hinged support case. The values start to correspond with the experimental results at a load of 16 kN, when the formation of plastic hinges in the fasteners is completed.

The maximum allowable deflection  $f_{\mathcal{U}}$  = 5 mm is reached at a load ranging from 15.7 to 17.2 kN, which represents 50.8 to 55.7 % of the load-bearing capacity and corresponds to a deflection of 4.8 to 5.3 mm as determined analytically for the hinged support case, and a deflection of 1.0 to 1.1 mm as determined analytically for the rigid fixation case.

It is evident that the deflection values determined analytically for the rigid fixation case are significantly lower than the actual deflections in the structure. Therefore, it is recommended to perform an analytical calculation of the panel's deflections under external load for the hinged support case.

#### 4. Conclusions

As a result of the study, the following outcomes were achieved:

- 1. It is shown that the loss of the load-bearing capacity of the panel happens due to bearing of the steel sheet of the web of the panel LGSP.
- 2. The method of calculating the bearing capacity of LSCS panel-to-slab fastenings is proposed and substantiated. The analytically calculated destructive load 28.25 kN is 9.3 % less than experimentally obtained destructive load 30.9 kN.
- 3. It is shown that the rigidity of the LSCS panel fastenings varies from the one corresponding to the fixed-support calculation scheme to the one corresponding to the hinged-support calculation scheme. The behavior of the panel corresponds to the fixed-support calculation scheme before the load is 30 % of the value that gives the maximum allowable deflection, than the fasteners work as

- an finite stiffness support and turn into a plastic hinge when the load reaches 90 % of the abovementioned load.
- 4. It is proposed to use the hinged-support calculation scheme in design practice.
- 5. The results of the research are implemented into the LLC "Sovbi" (Russian Federation, Saint Petersburg) activity.

#### References

- Danilov, N.D., Fedotov, P.A., Tretyakov, E.S., Gerasimova, V.S. Comparison of Options of Different Types of External Walls of Buildings. Zhilishnoye Stroitel'stvo [Housing Construction]. 2019. 5. Pp. 43–47. DOI: 10.31659/0044-4472-2019-5-43-47
- 2. Wasim, M., Wang, K., Yuan, Z., Jin, M., Abadel, A., Nehdi, M.L. An Optimized Energy Efficient Design of a Light Gauge Steel Building. Case Studies in Construction Materials. 2023. 19. Article no. e02398. DOI: 10.1016/j.cscm.2023.e02398
- 3. Efimchenko, M.I. Problems and Prospects of Modern Panel Housing Construction. Inzhenernyye Issledovaniya [Engineering Research]. 2022. 4(9). Pp. 17–25. URL: https://eng-res.ru/archive/2022/4/No9.pdf (date of application: 17.02.2025).
- Nazmeeva, T., Sivokhin, A. Stress-Strain State of Attachment Point of Curtain Frame Wall with Cladding on the Basis of Steel Cold-Bent Profile. Industrial and Civil Engineering. 2018. 10. Pp. 41–44. URL: http://www.pgs1923.ru/ru/index.php?m=4&y=2018&v=10&p=05 (date of application: 17.02.2025).
- 5. Rybakov, V., Kozinets, G., Vatin, N. Lightweight Steel Concrete Structures Technology with Foam Fiber-Cement Sheets. Magazine of Civil Engineering. 2018. 6(82). Pp. 103–111. DOI: 10.18720/MCE.82.10
- Wang, L., Yang, X.-J., Li, Z.-Q., Yin, P., Zhou, X.-F., Hu, Q. (2024) Experimental Study on the Interfacial Bonding Performance of Concrete-Filled Steel Tubes at Different Ambient Temperatures. Thin-Walled Structures, 205, 112368. DOI: 10.1016/j.tws.2024.112368
- Fan, J.-H., Wang, W.-D., Shi, Y.-L., Zheng, L. Low-Cycle Fatigue Behaviour of Concrete-Filled Double Skin Steel Tubular (CFDST) Members for Wind Turbine Towers. Thin-Walled Structures. 2024. 205(B). Article no. 112384. DOI: 10.1016/j.tws.2024.112384
- 8. Jamaluddin, N., Lam, D., Dai, X.H., Ye, J. An Experimental Study on Elliptical Concrete Filled Columns under Axial Compression. Journal of Constructional Steel Research. 2013. 87. Pp. 6–16. DOI: 10.1016/j.jcsr.2013.04.002
- 9. Dai, X., Lam, D. Numerical Modelling of the Axial Compressive Behaviour of Short Concrete-Filled Elliptical Steel Columns. Journal of Constructional Steel Research. 2010. 66(7). Pp. 931–942. DOI: 10.1016/j.jcsr.2010.02.003
- 10. Qiao, W., Zhang, X., Zhang, H., Zhang, L., Feng, H. Test Study on Eccentric Compression of Light Steel Concrete L-Shaped Composite Column in Modular Wall Prefabricated Building. Journal of Constructional Steel Research. 2024. 215. Article no. 108514. DOI: 10.1016/j.jcsr.2024.108514
- 11. Wang, X., Cheng, C., Wang, S., Wang, W. Study on the Flexural Behaviour of the Concrete Filled Square Steel Tube Beam with the Basic Magnesium Sulfate Cement-Based Composite Shell System. Construction and Building Materials. 2024. 424. Article no. 135968. DOI: 10.1016/j.conbuildmat.2024.135968
- 12. Cortés-Puentes, W.L., Palermo, D., Abdulridha, A., Majeed, M. Compressive Strength Capacity of Light Gauge Steel Composite Columns. Case Studies in Construction Materials. 2016. 5. Pp. 64–78. DOI: 10.1016/j.cscm.2016.08.001
- 13. Brian, Uy. Strength of Concrete Filled Steel Box Columns Incorporating Local Buckling. Journal of Structural Engineering. 2000. 126(3). Pp. 341–352. DOI: 10.1061/(ASCE)0733-9445(2000)126:3(341)
- Güldür, H., Baran, E., Topkaya, C. Experimental and Numerical Analysis of Cold-Formed Steel Floor Trusses with Concrete Filled Compression Chord. Engineering Structures. 2021. 234. Article no. 111813. DOI: 10.1016/J.ENGSTRUCT.2020.111813
- 15. Wang, J., Zhou, T., Wu, H., Guan, Y., Zhang, L. Cyclic Performance of Steel Frame Fabricated with Cold-Formed Steel Composite Wall Structure. Engineering Structures. 2022. 270. Article no. 114892. DOI: 10.1016/j.engstruct.2022.114892
- Chen, D., Wang, J., Pan, M., Zhou, J. Tests on Vertical Bearing Capacity of Steel-Foamed Concrete-Fiber Cement Pressure Plate Composite Walls. Shenyang Jianzhu Daxue Xuebao (Ziran Kexue Ban)/Journal of Shenyang Jianzhu University (Natural Science). 2018. 34(2). Pp. 275–285. DOI: 10.11717/j.issn:2095-1922.2018.02.10
- 17. Rassouli, B., Shafaei, S., Ayazi, A., Farahbod, F. Experimental and Numerical Study on Steel-Concrete Composite Shear Wall Using Light-Weight Concrete. Journal of Constructional Steel Research. 2016. 126. Pp. 117–128. DOI: 10.1016/j.jcsr.2016.07.016
- Yu, F., Kuang, G., Bu, S., Chen, L. Flexural Performance Tests and Numerical Analysis of Fabicated Light-Gauge Steel Reinforced Foam Concrete Filled Steel Mesh Formwork Wallboards. Structures. 2024. 66. Article no. 106813. DOI: 10.1016/j.istruc.2024.106813
- Rybakov, V. Condition Load Effect Factor of Profile Steel in Lightweight Steel Concrete Structures. Construction of Unique Buildings and Structures. 2020. 4(89). Article no. 8907. DOI: 10.18720/CUBS.89.7. 2023. 1(106). Article no. 10602. DOI: 10.4123/CUBS.106.2
- Xu, Y., Zhou, X., Shi, Y., Zou, Y., Xu, L., Xiang, Y., Ke, Ke. Lateral Resistance of OSB Sheathed Cold-Formed Steel Shear Walls. Thin-Walled Structures. 2021. 161. Article no. 107451. DOI: 10.1016/j.tws.2021.107451
- Rybakov, V., Seliverstov, A., Vakhidov, O. Fire Resistance of Lightweight Steel-Concrete Slab Panels under High-Temperature Exposure. E3S Web of Conference. 2021. 264. Article no. 02003. DOI: 10.1051/e3sconf/202126402003
- 22. Xiang, G., Song, D., Li, H., Zhou Y., Wang H., Shen G., Zhang, Z. Preparation of Steel Slag Foam Concrete and Fractal Model for Their Thermal Conductivity. Fractals. 2023. 7(8). Article no. 585. DOI: 10.3390/fractalfract7080585
- Kinoshita, T., Shintani, Y., Okazaki, T., Nishimura, T. Liew, J.Y.R. Effect of Steel-Fiber Reinforced Concrete on the Fire Resistance of Concrete-Filled Steel Tubular Columns under Simultanious Axial Loading and Double Curvative Bending. 11<sup>th</sup> International Conference on Structures in Fire (SiF2020). The University of Queensland. Brisbane, 2020. Pp.113–123. DOI: 10.14264/4767f7d
- 24. Zhuang, L.-D., Tao, M.-X., Zhao, J.-Z., Yang, K.-Y. Experimental and Numerical Investigations on the Mechanical Behaviour of Large-Span Circular Steel-Concrete Composite Slabs for Wind Power Tower. Thin-Walled Structures. 2024. 202. Article no. 112107. DOI: 10.1016/j.tws.2024.112107

- Rybakov, V., Seliverstov, A., Usanova, K. Steel Profile Corrosion Resistance in Contact with Monolithic Foam Concrete. E3S Web of Conferences. 2023. 365. Article no. 02001. DOI: 10.1051/e3sconf/202336502001
- Guan, Y., Zhou, X.-H., Shi, Y., Yao, X.-M. Experimental Study and Theoretical Analysis of Out-of-Plane and In-Plane Stiffness of Cold-Formed Thin-Walled Composite Floor. Gongcheng Lixue/Engineering Mechanics. 2023. 40(10). Pp. 21–32. DOI: 10.6052/j.lssn.1000-4750.2022.01.0079
- 27. Yang, N., Bai, F., Liu, W., Ge, H. Unified Static-Fatigue Bearing Design Model for Self-Tapping Screw Joints in Light-Weight Steel Roofs under Typhoon Hazard I. Journal of Southeast University (Natural Science Edition). 2024. 54(1). Pp. 67–71. DOI: 10.3969/j.lssn.1001-0505.2024.01.009
- 28. Yang, N., Liu, W., Bai, F., Ge, H. Research on Time-Varying Reliability of Self-Tapping Screw Joints of Light-Weight Steel Roofs under Typhoon. Hunan Daxue Xuebao/Journal of Hunan University Natural Sciences. 2021. 48(11). Pp. 72–81. DOI: 10.16339/j.Cnki.Hdxbzkb.2021.11.008
- 29. Kurazhova, V.G., Nazmeeva, T.V. Node Connections of Cold-Formed Steel Structures. Magazine of Civil Engineering. 2011. 3. Pp. 47–52. URL: https://engstroy.spbstu.ru/userfiles/files/2011/3(21)/kurazhova\_uzly.pdf (date of application: 17.02.2025).
- 30. Katranov, I.G. Tensile Testing and Calculation of Screw Joints of Light Thin-Walled Steel Structures. Vestnik MGSU [The Bulletin of Moscow State University of Construction]. 2010. 2. Pp. 89–93. URL: https://cyberleninka.ru/article/n/ispytaniya-i-raschet-vintovyh-soedineniy-legkih-stalnyh-tonkostennyh-konstruktsiy-na-rastyazhenie-1/viewer (date of application: 17.02.2025).
- 31. Wang, J., Qiu, Z., Liang, J. Experimental Investigations on the Lateral Performance of Foam Concrete Light Steel Keel Composite Wall. Journal of Building Engineering. 2023. 72. Article no. 106551. DOI: 10.1016/j.jobe.2023.106551

#### Information about the authors:

Vladimir Rybakov, Doctor of Technical Sciences ORCID: <a href="https://orcid.org/0000-0002-2299-3096">https://orcid.org/0000-0002-2299-3096</a>

E-mail: fishermanoff@mail.ru

Kseniia Usanova, PhD in Technical Sciences ORCID: https://orcid.org/0000-0002-5694-1737

E-mail: plml@mail.ru

Anatoly Seliverstov,

ORCID: https://orcid.org/0000-0001-9735-9615

E-mail: sovbitex@mail.ru

Alexandra Kislitcyna,

ORCID: https://orcid.org/0000-0003-4310-2069

E-mail: alexandra.ak.13@gmail.com

Anna Tsvetkova,

ORCID: https://orcid.org/0000-0002-2993-6836

E-mail: annatsvetkova2014@mail.ru

Stanislav Akimov,

https://orcid.org/0000-0002-2908-4565

E-mail: akimov sv@spbstu.ru

Received 22.09.2024. Approved after reviewing 24.11.2024. Accepted 06.12.2024.